Reliability of Predicting damage in hard rock mass around deep tunnels in terms of its convergence

Rodolfo Cabezas G.
SRK Consulting, Santiago, Chile

Adeline Delonca
Universidad Técnica Federico Santa María, Santiago, Chile

ABSTRACT: In deep excavations, mechanical instabilities may appear, inducing damage to the rock mass. These instabilities may be difficult to identify but are inferred as convergence of the walls over time. This magnitude and evolution may provide valuable information for tunnel stability analysis, as the extent of the damage affects where the ground support is installed. This study proposes a simple model to relate convergence with the depth of failure within the rock mass. A normalized damage curve is obtained as a function of the total deformation measured, for compressed and tensile areas around the excavation. The parameters are defined according to the stress state and the strength properties of the rock mass. The influence of the variability of the properties is considered, extending the analysis to a probabilistic case using Montecarlo method and obtaining reliability ranges for different rock masses expected in deep orebodies, for example in hydrothermally altered conditions.

Keywords: Deep mining, tunneling, Damage, Depth of failure, Reliability.

1 INTRODUCTION

When stress redistribution due to excavations surpasses rock mass strength, brittle failure can occur. In hard rock masses those mechanical instabilities may appear such as overbreak, collapsing, fault activation, spalling or seismicity, among others. Those phenomena are seen as an induced damage in the surrounding rock mass and can be noticed as a convergence of the walls over time (Karampinos, Hadjigeorgiou, Turcotte, & Mercier-Langevin, 2015). In practical terms, convergence is the consequence of mobilization and degrading of the rock mass and its interaction with ground support (Pardo, Villaescusa, Beck, & Brzovic, 2012; Rojat, Labiouse, Kaiser, & Descoeudres, 2009; Zhang et al., 2016). Convergence measurements are often recorded in projects but in most cases are dismissed after reaching an equilibrium condition, that indicates a safe operation of the tunnel (Martin, Chandler, & Read, 1996). Although a safe equilibrium may have been accepted, this does not mean that rock mass is undamaged and the possibility of a progressive failure in the short to long-term must not be discarded (Xia, Li, Li, Liu, & Yu, 2013).

In order to estimate the damage behavior and its extension inside the rock mass, this study analyzes several cases for convergence and estimated rock mass behavior and depth of failure (DoF).

This work leads to a simple formulation for the decrease of damage inside the rock mass, presented and related to in-situ deformations. To consider the influence of the properties variability, the analysis was extended to a probabilistic analysis using the Monte Carlo method and reliability ranges for different field stress and rock strength scenarios were obtained.

2 METHODOLOGY

2.1 Previous Studies

The presented work is based on previous studies, resume here. A scheme of the behavior near the excavation is shown in Figure 1 (a). The rock mass has a peak strength, and if it is surpassed, a Highly Damaged Zone (HDZ) and post-peak strength are reached. Less damage reaches up to the Excavation damaged zone (EDZ), which means that peak strength has been surpassed but more strain (Critical Plastic Strain, CPS) is required to reach the post-peak condition (Perras & Diederichs, 2016). The damage extension inside the rock mass and how it affects the volume where ground support is installed may provide accessible and valuable in-situ information of tunnel behavior, as shown in Figure 1 (b) (Espinoza & Landeros, 2014). Near the free boundary, the confining stress tends to zero and the ground support increases the internal pressure slightly. After in-situ assessment (Walton et al., 2015) and numerical modeling (Cabezas & Vallejos, 2022), a simplified function for the normalized damage can be validated, as shown in Figure 1 (c), according to AIC criterion (Akaike, 1974):

$$AIC = 2 \cdot k - n \cdot \ln(SS/n) \tag{1}$$

Where k is the number of parameters, n sample-size and SS is the sum of square-error. Then, the criterion captures the trade-off between the number of parameters and fit, and the optimal model is which minimizes the AIC value.

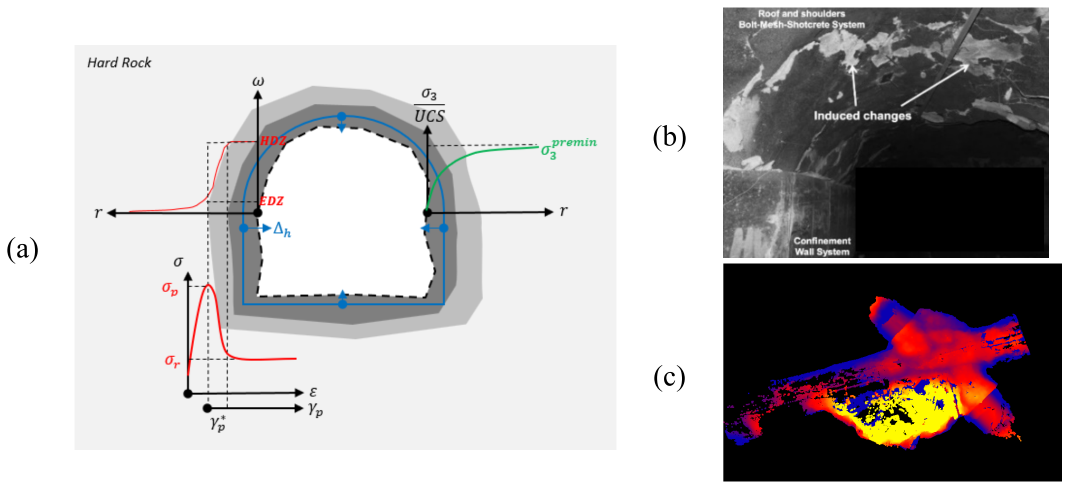

Figure 1. Damage distribution around excavations and induced changes (a) stress redistribution and brittle failure. (b) Visualization of induced damage in practice (after Espinosa & Landeros, 2014). (c) Example of convergence monitoring in drawpoint.

Although in practice transition between HDZ and EDZ tends to a discrete form, for estimating the damage decrease a continuous sigmoidal formulation in terms of normalized parameters was assumed, which may be expressed as:

$$\frac{D}{D_{max}} = \frac{1}{1 + \left(C_\sigma \cdot \left(\frac{r}{a}\right)\right)^{C_{RM}}} \tag{2}$$

Where D_{max} is maximal damage (convergence measurement) at tunnel surface, r is depth within the rock mass, a is tunnel radius, and C_σ and C_{RM} are fitting parameters, depending on field stress and rock mass strength, respectively (Cabezas & Vallejos, 2019). Figure 2 shows a scheme of the proposed fit function in (a) and (b) a generic case and a sensibility of its fitting parameters, and (c) calibration of the fit function for the estimated depths of failure (adapted from Walton et al. (2015) and Perras & Diederichs, 2016).

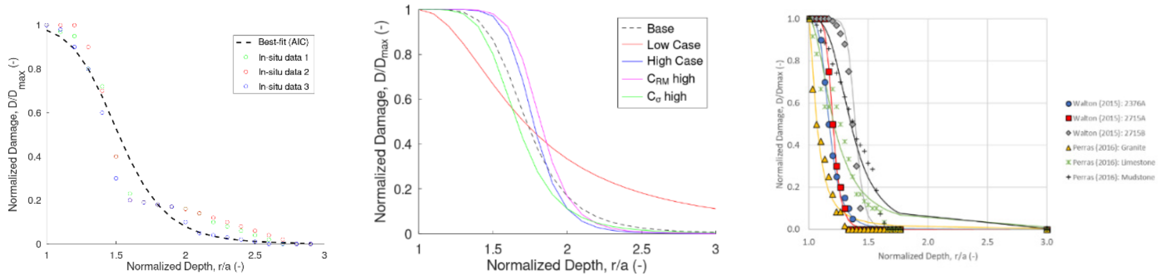

(a) (b) (c)

Figure 2. Sigmoidal function for estimating damage decay inside the rock mass. (a) Scheme for a best-fit of damage behavior (after Cabezas & Vallejos, 2019) (b) Generic sigmoidal function and analysis of the effect of fitting parameters. (c) Best-fit for calibration cases (Cabezas & Vallejos, 2019).

3 RELIABILITY ANALYSIS

3.1 Case Studies

As the Depth of Failure (DoF) and the observed overbreak do not have a unique value for similar conditions in the tunnel, a Monte Carlo simulation was conducted with literature data as follows. For that, considering different tunnels and lithologies, a database of depths, expected values, and ranges of variation is generated. The Figure 3 shows (a) differences between what was predicted and what was observed (Rojat et al., 2009) as well as (b) the variability for the same HDZ-EDZ model (Day, 2019). Three base cases were studied along with its stress field scenarios, and for each case a calibration parameter dataset was found using Eqs. (1) and (2).

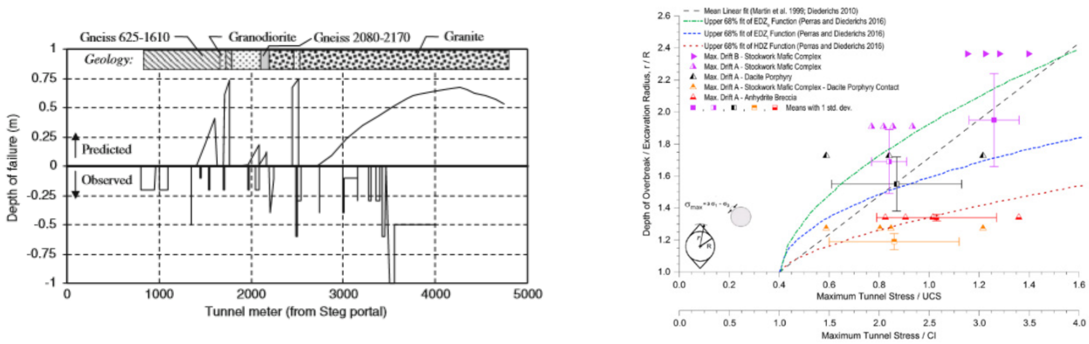

(a) (b)

Figure 3. Examples of variability observed in different tunneling projects. (a) Differences between predicted and observed overbreak (Rojat et al., 2009). (b) Variability for hydrothermally and intrusive environments (Day, 2019).

3.2 Loading and rock mass scenarios

To complement the previous analysis, other loadings and rock mass condition scenarios were analyzed, in particular:

a) Base cases: 3 main lithologies have enough data and were used as base cases (veined rock mass with medium strength infill, porphyry, and breccia).
b) Dynamic loading (induced seismicity): the damaged zone has been increased after including an explicit seismic (medium energy) signal using the software Flac 2D (Itasca, 2020). For the strength envelope, the conventional Hoek-Brown failure criterion and damping were applied.
c) Weaker rock mass condition: as former theory considers brittle hard-rock mass, a simulation with discrete fracture network (DFN) was added to model the increase of DoF that does not include them in brittle rock mass. Numerical simulation was conducted with ADFNE software (Alghalandis, 2017), and the DFN generation was heterogeneous around the tunnel in order to decrease the GSI value by 10 points.

4 RESULTS

Figure 4 shows an example of the fit results for the breccia case, where the simulation is conducted for the C_σ and C_{RM} parameters using a normal distribution. As the stresses are redistributed and the behavior of the tunnel is different if it is in the zone that destresses or in the zone that compresses, in (a) the adjustments for both cases are shown, as well as the extension in case of seismicity and more jointed rock; while in (b) the representative envelopes are obtained for P30 (optimistic, lower extent of damage), P50 (expected), and P70 (pessimistic, greater extent of damage).

It can be seen that the base case can reduce its extent by about 10% in a favorable case, while it can increase up to 20% in pessimistic cases. This phenomenon is also in found in other cases, reaching up to 30% in cases of roof destressing, due to the influence of minor wedges.

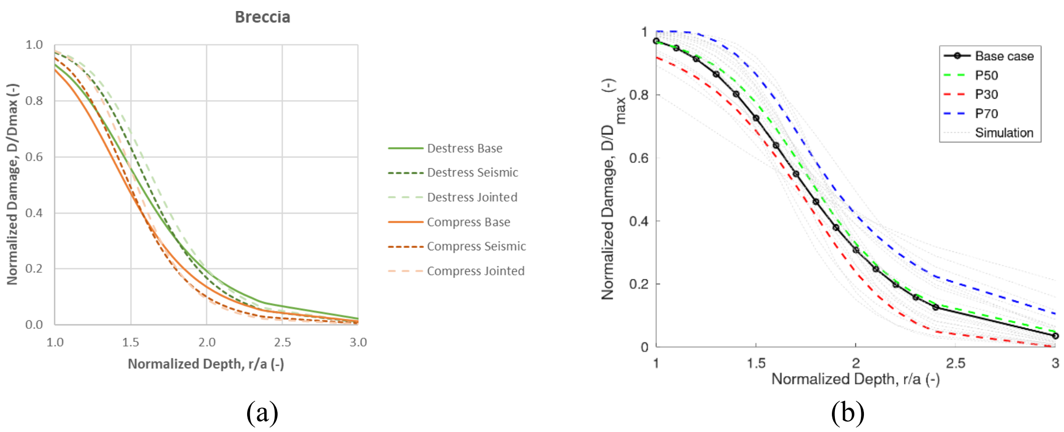

Figure 4. Example of Monte Carlo modeling for different scenarios. (a) Simulation and characteristic parameters (P30, P50, P70). (b) Application for breccia specific base case.

4.1 Proposal for Caving and Deep Tunnels

To extend its use to deep mining, Table 1 summarizes the parameters obtained from the calibration and its subsequent simulation. Then, Figure 4 presents the comparison between lithologies and field stress scenarios.

Table 1. Best-fit for normalized sigmoidal damage estimation considering 3 main rock mass cases and stress zones around the tunnel: Destressing tend to be located at the walls, while Compressive tend to be located at the roof.

							Base Case		**Seismic Case**		**Heterogeneous Joints Case**	
Lithology	GSI (–)	UCS (–)	σ_1 (MPa)	σ_2 (MPa)	σ_3 (MPa)	Stress zone around tunnel	C_σ (–)	C_{RM} (–)	C_σ (–)	C_{RM} (–)	C_σ (–)	C_{RM} (–)
Veined	60-65	100	56	45	32	Destress	0.57	6.2	0.54	8.8	0.53	13.8
						Compress	0.58	8.0	0.56	7.9	0.55	10.0
Porphyry	65-70	110	60	42	32	Destress	0.68	7.7	0.67	10.3	0.66	11.6
						Compress	0.68	8.6	0.67	8.9	0.66	13.4
Breccia	60-65	90	60	42	32	Destress	0.64	5.8	0.62	7.4	0.60	7.6
						Compress	0.68	6.0	0.67	7.5	0.65	8.7

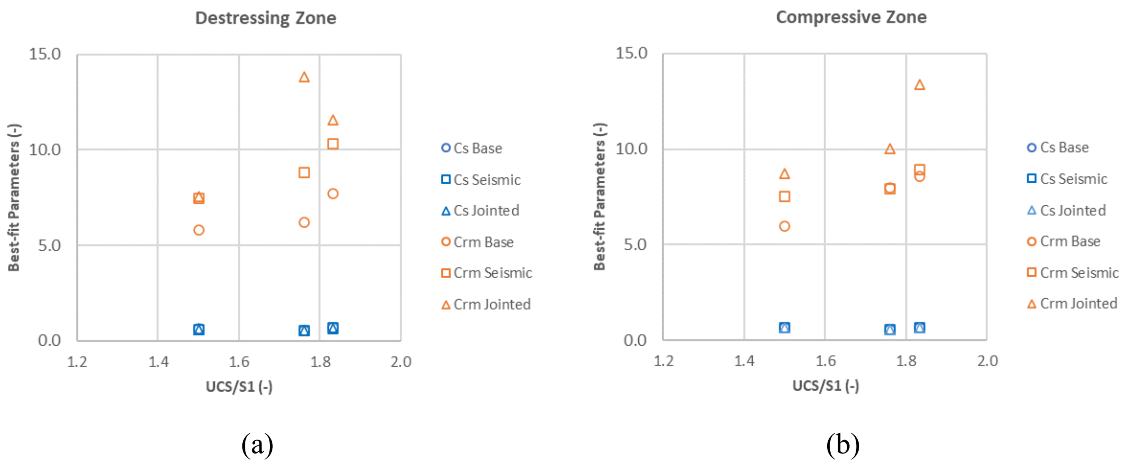

Figure 5. Sigmoidal function parameters (C_σ and C_{RM}) in terms of the stress/strength ratio for all analyzed cases. (a) In case of destressing zones around the tunnel (mostly walls). (b) In case of compressive zone around the tunnel (Mostly roof).

Then, it is possible to estimate to other parameters based on the stress ratio (σ_1/UCS), such as for C_σ it tends to a constant value (lower influence), and for C_{RM} may be estimated as:

$$C_{RM}^{Dest} = 4.6 \cdot \frac{UCS}{\sigma_1} - 1.23$$
$$C_{RM}^{Comp} = 7.7 \cdot \frac{UCS}{\sigma_1} - 5.65 \quad (3)$$

Finally, it can be extended towards the convergence of tunnels considering that they are linked and proportional phenomena, such as:

$$u_r\left(\frac{r}{a}\right) = u_{r=0}^{max} \cdot D\left(\frac{r}{a}, C_\sigma, C_{RM}\right) \quad (4)$$

5 CONCLUSIONS

A normalized damage curve was defined as a function of the total deformation measured, both for compressed and destressed areas around deep tunnels, such as the parameters are defined according to the stress state and the strength properties of the rock mass. In addition, the influence of the variability of the properties is considered, extending the analysis to a probabilistic case using the Monte Carlo method and obtaining reliability ranges for different rock masses. In terms of the base case, its extent can be reduced by about 10% in a favorable case, while it can increase up to 20% in pessimistic cases. Besides, it is possible to project to other cases based on the stress ratio, towards to obtain the depth of damage in terms of the superficial convergence.

REFERENCES

Akaike, H. (1974). A new look at the statistical model identification. IEEE Trans Autom Control, 19 (6), pp. 716-723. http://doi.org/10.1109/TAC.1974.1100705

Alghalandis, Y. (2017). ADFNE: Open source software for discrete fracture network engineering, two and three dimensional applications. Computers & Geosciences, 102, pp. 1-11. https://doi.org/10.1016/j.cageo.2017.02.002

Cabezas, R. & Vallejos, J. (2019). A criterion for the extent of damage around excavated brittle hard rock masses in terms of its convergence over time. In 14th International Congress of Rock Mechanics and Rock Engineering. Iguazú, Brazil.

Cabezas R. & Vallejos, J. (2022). Nonlinear criterion for strength mobilization in brittle failure of rock and its extension to the tunnel scale, International Journal of Mining Science and Technology, https://doi.org/10.1016/j.ijmst.2022.04.002

Day, J. (2019) Brittle overbreak prediction in deep excavations for hydrothermally altered and heterogeneous rockmasses. Bull Eng Geol Environ 79, 1041–1060. https://doi.org/10.1007/s10064-019-01578-z

Espinosa, A., & Landeros, P. (2014). Implementation of LiDAR technology to evaluate deformation field induced by panel caving exploitation, Codelco Chile El Teniente Division. In R. Castro (Ed.), 3rd International Symposioum on Block and Sub Level Caving (pp. 394–402). Santiago, Chile

Karampinos, E., Hadjigeorgiou, J., Turcotte, P., & Mercier-Langevin, F. (2015). Large-scale deformation in underground hard-rock mines. Journal of the Southern African Institute of Mining and Metallurgy, 115(7), 645–652. https://doi.org/10.17159/2411-9717/2015/v115n7a11

Martin, C. D., Chandler, N. A., & Read, R. S. (1996). The role of convergence measurements in characterizing a rock mass. Canadian Geotechnical Journal, 33(2), 363–370. https://doi.org/10.1139/t96-014

Pardo, C., Villaescusa, E., Beck, D., & Brzovic, A. (2012). Back Analysis of Intensive Rock Mass Damage at the El Teniente Mine. In CRC Conference.

Perras, M., & Diederichs, M. (2016). Predicting excavation damage zone depths in brittle rocks. Journal of Rock Mechanics and Geotechnical Engineering2, 8, 60–74. https://doi.org/10.1016/j.jrmge.2015.11.004

Rojat, F., Labiouse, V., Kaiser, P., & Descoeudres, F. (2009). Brittle rock failure in the Steg Lateral Adit of the Lotschberg Base Tunnel. Rock Mechanics and Rock Engineering, 42, 341–359. https://doi.org/10.1007/s00603-008-0015-z

Walton, G., Lato, M., Anschütz, H., Perras, M. A., & Diederichs, M. S. (2015). Non-invasive detection of fractures, fracture zones, and rock damage in a hard rock excavation — Experience from the Äspö Hard Rock Laboratory in Sweden. Engineering Geology, 196, 210–221. https://doi.org/10.1016/j.enggeo.2015.07.010

Xia, X., Li, H. B., Li, J. C., Liu, B., & Yu, C. (2013). A case study on rock damage prediction and control method for underground tunnels subjected to adjacent excavation blasting. Tunnelling and Underground Space Technology, 35, 1–7. https://doi.org/10.1016/j.tust.2012.11.010

Zhang, J. C., Xu, W. Y., Wang, H. L., Wang, R. B., Meng, Q. X., & Du, S. W. (2016). A coupled elastoplastic damage model for brittle rocks and its application in modelling underground excavation. International Journal of Rock Mechanics and Mining Sciences, 84, 130–141. https://doi.org/10.1016/j.ijrmms.2015.11.011